JB
Journals.ASM.org

Identification and Characterization of Mutations Conferring Resistance to D-Amino Acids in *Bacillus subtilis*

Sara A. Leiman,[a] Charles Richardson,[b] Lucy Foulston,[a] Alexander K. W. Elsholz,[a] Eric A. First,[b] Richard Losick[a]

Department of Molecular and Cellular Biology, Harvard University, Cambridge, Massachusetts, USA[a]; Department of Biochemistry and Molecular Biology, Louisiana State University Health Sciences Center in Shreveport, Shreveport, Louisiana, USA[b]

ABSTRACT

Bacteria produce D-amino acids for incorporation into the peptidoglycan and certain nonribosomally produced peptides. However, D-amino acids are toxic if mischarged on tRNAs or misincorporated into protein. Common strains of the Gram-positive bacterium *Bacillus subtilis* are particularly sensitive to the growth-inhibitory effects of D-tyrosine due to the absence of D-aminoacyl-tRNA deacylase, an enzyme that prevents misincorporation of D-tyrosine and other D-amino acids into nascent proteins. We isolated spontaneous mutants of *B. subtilis* that survive in the presence of a mixture of D-leucine, D-methionine, D-tryptophan, and D-tyrosine. Whole-genome sequencing revealed that these strains harbored mutations affecting $tRNA^{Tyr}$ charging. Three of the most potent mutations enhanced the expression of the gene (*tyrS*) for tyrosyl-tRNA synthetase. In particular, resistance was conferred by mutations that destabilized the terminator hairpin of the *tyrS* riboswitch, as well as by a mutation that transformed a $tRNA^{Phe}$ into a *tyrS* riboswitch ligand. The most potent mutation, a substitution near the tyrosine recognition site of tyrosyl-tRNA synthetase, improved enzyme stereoselectivity. We conclude that these mutations promote the proper charging of $tRNA^{Tyr}$, thus facilitating the exclusion of D-tyrosine from protein biosynthesis in cells that lack D-aminoacyl-tRNA deacylase.

IMPORTANCE

Proteins are composed of L-amino acids. Mischarging of tRNAs with D-amino acids or the misincorporation of D-amino acids into proteins causes toxicity. This work reports on mutations that confer resistance to D-amino acids and their mechanisms of action.

Almost all bacteria produce and utilize D-amino acids (1, 2). The peptidoglycan typically contains the D-amino acids D-Ala and D-Glu. However, many bacteria produce other (noncanonical) D-amino acids as well (1). For example, *Vibrio cholerae* produces D-Met and D-Leu, which can regulate peptidoglycan synthesis (1, 3). Also, lipoteichoic and wall teichoic acids are modified with D-Ala, and D-amino acids are incorporated into nonribosomally synthesized peptides, such as the *Bacillus subtilis* lipopeptides surfactin (containing D-Leu) and iturin A (containing D-Asn and D-Tyr) (4, 5). For bacteria to exploit D-amino acids effectively, they must also prevent misincorporation of D-amino acids into proteins, as this would cause proteotoxicity (6, 7). Most D-amino acids are eliminated from the translation machinery by L-stereospecific aminoacyl-tRNA synthetases (8). However, tyrosyl-tRNA synthetase (TyrRS) cannot effectively distinguish between L-Tyr and D-Tyr, making D-Tyr potentially toxic to cells (8). In many organisms, D-Tyr toxicity is mitigated by a D-aminoacyl-tRNA deacylase, encoded by *dtd*, which prevents D-Tyr from sequestering $tRNA^{Tyr}$ or being incorporated into protein (9–11).

Recently, we found that the standard *B. subtilis* laboratory strains 3610 and 168 contain a mutated form of *dtd*, rendering them highly sensitive to D-Tyr toxicity. However, strains in which *dtd* was repaired were resistant to millimolar levels of D-amino acids (12). Moreover, a dtd^+ derivative of strain 3610 formed robust biofilms in the presence of D-amino acids, exhibiting an approximately 10,000-fold increase in resistance compared to the parental strain. This finding indicated that previous reports of biofilm inhibition by D-Tyr actually reflect a D-Tyr-induced growth defect (12). In the present investigation, we sought to identify additional genes involved in resistance to D-amino acids. We isolated and analyzed seven mutants that exhibit resistance to D-amino acids and compared their growth and biofilm phenotypes to those of the parental strain 3610. Our results offer additional insights into how *B. subtilis* strains lacking D-aminoacyl-tRNA deacylase activity can overcome exposure to D-amino acids and prevent proteotoxicity.

MATERIALS AND METHODS

Strains and growth conditions. *Bacillus subtilis* NCIB3610 or 168 and *Escherichia coli* Turbo (New England BioLabs, USA) or DH5α were grown in Luria-Bertani (LB) broth (10 g tryptone per liter, 5 g yeast extract per liter, 5 g NaCl per liter) or on LB agar plates containing 1.5% Bacto agar at 37°C. When appropriate, 1 μg/ml erythromycin and 25 μg/ml lincomycin, 5 μg/ml chloramphenicol, or 100 μg/ml ampicillin were added to liquid or solid medium. Strains used in this study are listed in Table S1 in the supplemental material.

Mutant isolation and identification. Spontaneous mutants resistant to D-amino acids were isolated by growing *B. subtilis* 3610 on solid LB

Received 8 January 2015 Accepted 19 February 2015
Accepted manuscript posted online 2 March 2015
Citation Leiman SA, Richardson C, Foulston L, Elsholz AKW, First EA, Losick R. 2015. Identification and characterization of mutations conferring resistance to D-amino acids in *Bacillus subtilis*. J Bacteriol 197:1632–1639. doi:10.1128/JB.00009-15.
Editor: P. de Boer
Address correspondence to Richard Losick, losick@mcb.harvard.edu.
Supplemental material for this article may be found at http://dx.doi.org/10.1128/JB.00009-15.

doi:10.1128/JB.00009-15

medium supplemented with D-leucine, D-methionine, D-tryptophan, and D-tyrosine (D-LMWY), each at 500 μM. The frequency at which mutations conferring resistance arose was calculated by plating dilutions on solid LB medium alone or supplemented with 500 μM D-LMWY. Genomic DNA libraries for whole-genome sequencing were prepared using the NEBNext kit according to the manufacturer's instructions. Individual barcodes for multiplexed sequencing were supplied by Illumina.

Strain construction. Strains were constructed as described in the supplemental material, using standard procedures (13, 14). All strains, primers, and plasmids used in this study are listed in Table S1 in the supplemental material.

Biofilm assays. Colony biofilms were grown by spotting 2 μl of early-stationary-phase cultures on unmodified solid MSgg medium (15) or solid MSgg without L-FTW, as indicated in the text. D-Tyr was stored as a 10 mM stock solution in 0.1 M HCl and diluted to achieve the indicated final concentrations. Plates were incubated at 30°C, and photographs were taken after 72 h.

Growth measurements. Cells were grown to mid-exponential phase in MSgg medium, diluted to an optical density at 600 nm (OD_{600}) of 0.03 in fresh MSgg medium, and treated with 10 μM D-Tyr or an equivalent volume of distilled water (dH_2O). Aliquots of 250 μl were transferred to a Costar polystyrene 96-well plate with a low-evaporation lid (Fisher Scientific, USA). OD_{600} was measured every 10 min for 7 h in a BioTek Synergy 2 luminometer (BioTek, USA) with continuous medium shaking at 37°C.

Kinetic luciferase assay. Luciferase activity was tested as previously described (12).

TyrRS protein purification and kinetic analyses. Materials were obtained from the sources indicated: Arctic Express (DE3) *E. coli* cells, Agilent; Rosetta 2 (DE3) and BL21(DE3) *E. coli* cells, EMD Biosciences; His-Pur nickel-nitrilotriacetic acid (Ni-NTA) resin, Promega; Biosafe II scintillation cocktail, Research Products International Corporation; and L-[^{14}C]Tyr, Moravek. All other reagents were obtained from VWR International or Fisher Scientific. Curve fitting and graphing were performed using GraFit (Erithacus Software, Ltd., Horley, Surrey, United Kingdom) and Kaleidograph (Synergy Software, Reading, PA).

Plasmids for the expression of C-terminally His_6-tagged TyrRS (wild type and A202V variant) were constructed as follows. pET-28a (Novagen) was linearized with NcoI and XhoI such that the C-terminal His_6 tag was preserved but the N-terminal His_6 tag was removed. Primers 73 and 74 were used to amplify the fragment containing *tyrS* from *B. subtilis* 3610 chromosomal DNA. The resulting fragments were then joined in an isothermal assembly reaction (14) with linearized and gel-purified pET-28a to produce pSL006 (for the production of $TyrRS^{WT}$-His_6) or pSL007 (for the production of $TyrRS^{A202V}$-His_6). The plasmids were maintained in Arctic Express (DE3), Rosetta 2 (DE3), or BL21(DE3) *E. coli* cells using selection with kanamycin at 25 μg/ml. Plasmid inserts were verified by sequencing using primers 73 and 74.

To verify expression, BL21(DE3) cells harboring pSL006 or pSL007 were grown overnight at 37°C in 5 ml LB medium with kanamycin at 30 μg/ml. Overnight cultures were diluted 1:100 into fresh 25-ml LB medium with kanamycin at 50 μg/ml and grown at 37°C. When the cultures reached an optical density (600 nm) of 0.3 to 0.35, the cultures were either left untreated or treated with 500 μM or 1 mM isopropyl-β-D-1-thiogalactopyranoside (IPTG). After growth for 4 h at 30°C, aliquots were collected, pelleted, boiled, and run on an SDS-PAGE gel. Expression was confirmed by Western blotting as described previously (16), except that the primary antibody was rabbit anti-His_6 (ab9108; Abcam) used at a dilution of 1:5,000.

The AMP deaminase and IMP dehydrogenase were expressed in *E. coli* Rosetta 2 (DE3), and the inorganic pyrophosphatase, cyclodityrosine synthase, and D-aminoacyl-tRNA deacylase were expressed in *E. coli* BL21(DE3) cells, as described in the work of E. A. First (submitted for publication) and E. A. First and C. Richardson (submitted for publication). T7 RNA polymerase was isolated using standard procedures. The pET-28-based *B. subtilis* tyrosyl-tRNA synthetase wild-type- and A202V variant-encoding plasmids (pSL006 and pSL007) were transformed into Arctic Express (DE3) cells. Single colonies were grown in 5 ml 2× YT (16 g/liter tryptone, 10 g/liter yeast extract, and 5 g/liter NaCl) with 50 μg/ml kanamycin overnight at 37°C. Four 500-ml Delong flasks containing 2× YT with kanamycin were inoculated with 1 ml of overnight culture. Flasks were incubated at 37°C at 250 rpm in a platform shaker until the optical density at 600 nm was 0.4 to 0.6. Flasks were chilled for about 30 min before protein expression was induced with IPTG at a final concentration of 0.5 mM. Flasks were incubated at 13°C for at least 24 h prior to protein purification.

Recombinant enzymes were isolated using Ni-NTA affinity chromatography, as previously described (17). Both *B. subtilis* tyrosyl-tRNA synthetase wild type and A202V variant were initially dialyzed against buffer containing 0.1 mM inorganic pyrophosphate, followed by three more rounds of dialysis to remove pyrophosphate and released substrate. Proteins were isolated to >95% homogeneity based on SDS-PAGE. Extinction coefficients and molecular weights were calculated using the ExPASy ProtParam tool (18). Purified proteins were stored in the buffers described in the work of First and Richardson (submitted). Both *B. subtilis* tyrosyl-tRNA synthetase wild type and A202V variant were stored in 20 mM Tris, pH 7.8, 1 mM EDTA, 10 mM β-mercaptoethanol, and 50% (vol/vol) glycerol.

Geobacillus stearothermophilus $tRNA^{Tyr}$ was synthesized by runoff transcription using T7 RNA polymerase using pGFX-WT, as previously described (17).

The concentration of tyrosyl-tRNA synthetase was determined using a filter-based active site titration assay that monitors the formation of the enzyme-bound tyrosyl-adenylate intermediate complex in the absence of tRNA. Reaction mixtures contained 10 μM L-[^{14}C]Tyr, 10 mM Mg-ATP, 2 U/ml inorganic pyrophosphatase, and 1 to 5 μM enzyme being tested, based on A_{280} measurements, in 100 mM Tris (pH 7.8) and 10 mM $MgCl_2$. Reaction mixtures were incubated at 25°C, and samples were filtered over Protran BA-85 nitrocellulose discs presoaked with 100 mM Tris (pH 7.8) and 10 mM $MgCl_2$. Filters were washed three times with cold buffer, dried, and counted in 5.5 ml Biosafe II scintillation cocktail by a Beckman LS-6500 scintillation counter.

Real-time, continuous AMP detection assays were performed as elaborated in the work of First (submitted) and First and Richardson (submitted). Reaction mixtures contained 50 mM Tris (pH 7.78), 10 mM KCl, 0.1 mM dithiothreitol, 10 mM $MgCl_2$, 10 mM Mg-ATP, 5 mM NAD^+, 160 nM AMP deaminase, 640 nM IMP dehydrogenase, 2 U/ml inorganic pyrophosphatase, 5 nM to 0.5 mM TyrRS, and variable [$tRNA^{Tyr}$] and [Tyr]. NAD^+ and ATP solutions were adjusted to pH 7.0 prior to use. Assays were performed in a 96-well plate (100 or 200 μl per well) at 25°C by monitoring the change in absorbance at 340 nm (A_{340}) that occurs with the conversion of NAD^+ to NADH. This reaction provides a readout for the consumption of ATP to form AMP, which is converted to IMP and XMP by AMP deaminase and IMP dehydrogenase, respectively. Under these conditions, the formation of tyrosyl-$tRNA^{Tyr}$ is the rate-limiting step and the tRNA substrate is nonlimiting due to the addition of recycling enzymes: 8 μM cyclodityrosine synthase or 50 μM D-tyrosyl-$tRNA^{Tyr}$ deacylase for L- and D-Tyr, respectively. The values for K_m^{tRNA} and k_{cat} were obtained by varying the tRNA concentration under conditions where the L- or D-Tyr concentration is saturating (1 mM). The values for $K_m^{L\text{-}Tyr}$, $K_m^{D\text{-}Tyr}$, and k_{cat} were obtained by varying the L- or D-Tyr concentration under conditions where the tRNA concentration is saturating (i.e., 5 μM).

Initial rates were determined for each substrate concentration by a linear fit of a plot of A_{340} against time. K_m and V_{max} values were determined by subtracting the no-substrate rate and plotting the initial rate against substrate concentration and fitting the curve to the Henri-Michaelis-Menten equation: $v_o = V_{max}[S]/(K_m + [S])$, where K_m is the affinity for the substrate and v_o is the initial rate. The k_{cat} values were calculated by the equation $V_{max} = k_{cat}[E]$, where [E] is the molar concentration of the enzyme in the assay.

TABLE 1 Spontaneously arising mutations predicted to confer resistance to D-LMWY[a]

Gene	Nucleotide change	Amino acid change
tyrS	−38ΩC	NA
	−38C>T	NA
	605G>A	A202V
trnD-Phe	35A>T	NA
hrcA	−8A>G	NA
ppaC	234A>T	E78D
	434C>T	A145V
	Δ496–498 (GCA)	ΔA166

[a] Given positions are relative to the start of the open reading frame. NA, not applicable.

***tyrS* overexpression assay.** *B. subtilis* strains 3610, SLH69, and SLH70 were grown to early stationary phase in 3 ml LB medium, with shaking at 37°C, and 2 μl of each culture was spotted on MSgg agar, MSgg agar with 750 μM isopropyl-β-D-1-thiogalactopyranoside (IPTG), MSgg agar with 10 μM D-Tyr, or MSgg agar with both 750 μM IPTG and 10 μM D-Tyr. The plates were incubated at 30°C and photographed at 72 h.

RESULTS AND DISCUSSION

Spontaneous resistance to D-amino acids occurs with high frequency. Spontaneously arising mutants with resistance to growth inhibition by D-amino acids were selected on solid LB medium supplemented with 500 μM (each) D-leucine, D-methionine, D-tryptophan, and D-tyrosine (D-LMWY). Mutants arose at a frequency of about 10^{-6}, a high frequency that suggested that mutations at multiple loci were able to confer resistance. Indeed, whole-genome sequencing of seven spontaneous resistance mutants revealed eight distinct mutations: three mutations in the inorganic pyrophosphatase gene *ppaC*, three mutations in or upstream of the TyrRS gene *tyrS*, one mutation in the $tRNA^{Phe}$ encoded by *trnD-Phe*, and one mutation upstream of the protein chaperone repressor gene *hrcA* (Table 1) (19–22). Of the seven mutants analyzed, six harbored only one mutation, while one mutant (SLH15) harbored two mutations ($hrcA^{-8A>G}$ and $ppaC^{\Delta A166}$).

Identification of mutations conferring resistance to D-amino acids. Next, we constructed congenic derivatives of the parental strain 3610 that separately contained the mutations $ppaC^{A145V}$, $tyrS^{-38C>T}$, $tyrS^{A202V}$, $trnD\text{-}Phe^{35A>T}$, and $hrcA^{-8A>G}$. Growth curves (Fig. 1) and biofilm assays (Fig. 2) revealed that the mutations in *ppaC*, *tyrS*, and *trnD-Phe* conferred resistance to D-Tyr. These mutations conferred resistance as effectively against an equimolar mixture of D-LMWY as they did against D-Tyr (data not shown), consistent with our previous findings that D-Tyr is the only toxic component of this mixture at physiologically relevant concentrations (12). In contrast, the mutation upstream of *hrcA* was ineffective against D-amino acid stress (Fig. 1 and 2). Given that the original source of this mutation (SLH15) harbored a second mutation in *ppaC* ($ppaC^{\Delta A166}$), and accounting for our findings that a separate mutation in *ppaC* ($ppaC^{A145V}$) protects *B. subtilis* from D-Tyr toxicity, we infer that the active mutation of strain SLH15 is $ppaC^{\Delta A166}$.

It is interesting that mutations in the inorganic pyrophosphatase gene *ppaC* impart resistance to D-amino acids (Table 1 and Fig. 1 and 2). We speculate that these mutations do so by slowing the rate of nucleoside triphosphate (NTP)-driven reactions, including the charging (or mischarging) of tRNAs (21). We note

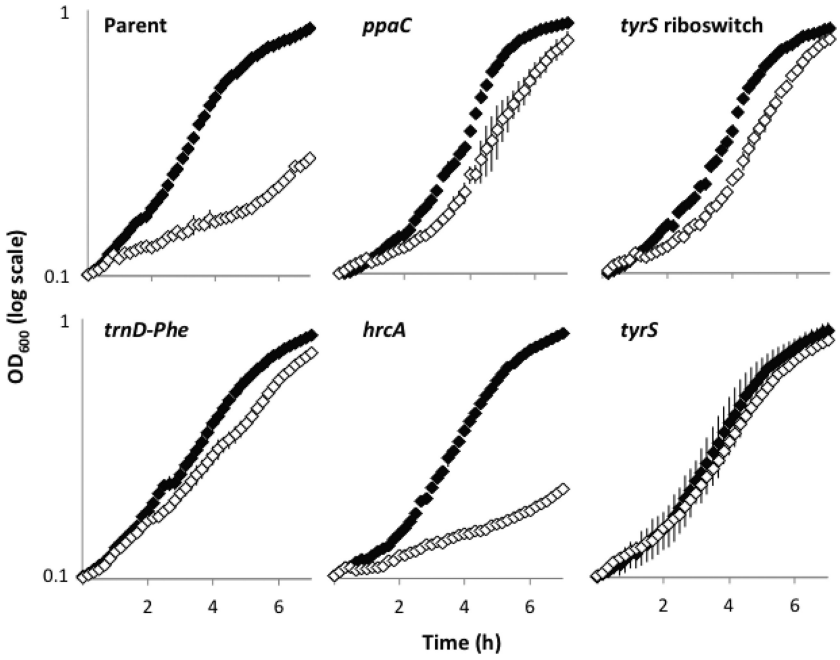

FIG 1 Mutations from spontaneously arising mutants confer resistance to growth inhibition by D-amino acids when moved to the parental strain. Optical density of cells grown in shaking MSgg medium was measured in the presence (white diamonds) or absence (black diamonds) of 10 μM D-Tyr. The $ppaC^{A145V}$, *tyrS* riboswitch ($tyrS^{-38C>T}$), $tyrS^{A202V}$, $trnD\text{-}Phe^{35A>T}$, and $hrcA^{-8A>G}$ mutants were constructed by reconstituting select spontaneously arising mutations (Table 1) in the parent strain 3610. Results are shown as a semilog plot and indicate the averages from four replicates. Error bars show the standard deviations.

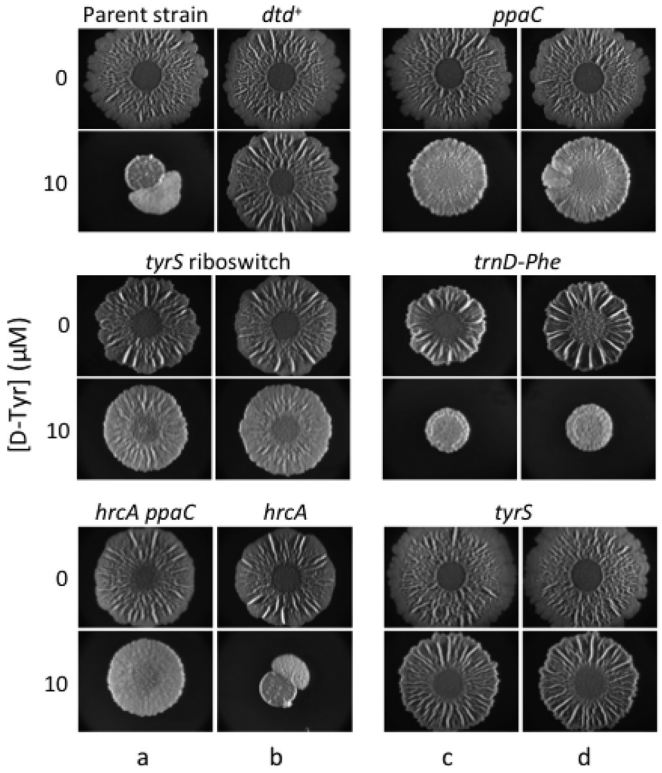

FIG 2 Congenic mutants exhibiting resistance to biofilm inhibition by D-amino acids. Spontaneous mutants (columns a and c) and their reconstituted counterparts (columns b and d) were spotted on solid MSgg medium alone or solid MSgg medium containing 10 μM D-Tyr. The reconstituted spontaneous mutants are as follows: $ppaC^{A145V}$, *tyrS* riboswitch ($tyrS^{-38C>T}$), $tyrS^{A202V}$, $trnD\text{-}Phe^{35A>T}$, and $hrcA^{-8A>G}$. The parental strain of the spontaneous mutants (3610, which is mutant for *dtd*) and a dtd^{+} strain (SLH31) are included as a negative control and positive control, respectively. Images were taken after 72 h of incubation at 30°C.

that Halonen et al. (21) previously constructed the $ppaC^{E78D}$ mutation in *B. subtilis* and that we recovered the same mutation in our selection for resistance to D-amino acids. The authors found that the E78D substitution enhanced the affinity of inorganic pyrophosphatase for its metal ion cofactor, Mn^{2+}, but simultaneously changed the metal ion specificity of the enzyme from Mn^{2+} to Mg^{2+} (21). We posit that these changes hamper the enzyme's efficiency and suggest that $ppaC^{A145V}$ and $ppaC^{\Delta A166}$ also confer resistance to D-amino acids by impairing inorganic pyrophosphatase activity. Furthermore, these changes may particularly disadvantage the mischarging of $tRNA^{Tyr}$ with D-Tyr. Kinetic analyses of a *B. subtilis* TyrRS homolog (*G. stearothermophilus* TyrRS) revealed that pyrophosphate (PP_i) binds to the TyrRS–D-Tyr-AMP complex with a 14-fold-higher affinity than that with which it binds to the TyrRS–L-Tyr-AMP complex (23). This difference contributed to the lower relative turnover rate for TyrRS bound to D-Tyr. *B. subtilis* TyrRS, which is 69% identical (and 89% similar) in protein sequence to *G. stearothermophilus* TyrRS, also exhibits a lower turnover rate for D-Tyr than for L-Tyr. Likely, the PP_i binding affinities of the *B. subtilis* TyrRS and the *G. stearothermophilus* TyrRS are similar. Thus, accounting for the higher binding affinity of the TyrRS–D-Tyr-AMP complex to PP_i, it is plausible that mildly reduced pyrophosphatase activity could preferentially disadvantage activation of D-Tyr by TyrRS and result in a reduction of $tRNA^{Tyr}$ mischarging.

$TyrRS^{A202V}$ is more stereoselective than is wild-type TyrRS. The most effective of the D-LMWY-resistant mutations was $tyrS^{A202V}$, which caused an amino acid substitution proximal to the tyrosine-binding site of TyrRS (20). Because A202 is located in an alpha helix, it is reasonable to suppose that introducing the branched amino acid valine at this position alters the geometry of the tyrosine-binding site. This hypothesis is supported by the crystal structures of a divergent and more stereoselective class of tyrosyl-$tRNA^{Tyr}$ synthetase known as TyrRZ, which demonstrate a correlation between the presence of a bulkier group at position 202 (Met or Val) and superior discrimination between L-Tyr and D-Tyr, as noted in reference 24 and the accompanying paper by Williams-Wagner et al. (25).

Surprisingly, wild-type *B. subtilis* TyrRS has a higher affinity for D-Tyr than it does for L-Tyr (K_m = 4 μM and 90 μM, respectively). In contrast, the turnover number (k_{cat}) for the wild-type enzyme is 60-fold higher for the L-stereoisomer, resulting in a specificity constant that favors L-Tyr over D-Tyr (k_{cat}/K_m = 0.173 for L-Tyr and 0.057 for D-Tyr) (Fig. 3; Table 2). Comparison of the wild type and the A202V variant of TyrRS indicated that the A202V substitution decreases the affinity of the enzyme 3-fold and 22-fold for L-Tyr and D-Tyr, respectively. As the k_{cat} values are unaffected by the A202V substitution, this translates to a 7-fold increase in the specificity of the TyrRS variant for L-Tyr. The second step of $tRNA^{Tyr}$ charging (the transfer of the aminoacyl group from aminoacyl-AMP to the tRNA) was not significantly affected by the A202V substitution (Fig. 3; Table 2). Since the L-Tyr binding site is distal to the $tRNA^{Tyr}$ binding site, we infer that the A202V substitution does not induce widespread conformational changes in the protein structure (20). These results indicate that *B. subtilis* $TyrRS^{WT}$ is a poor discriminator between L-Tyr and D-Tyr due to its higher binding affinity for D-Tyr (K_m = 4 μM) than for L-Tyr (K_m = 90 μM). D-Tyr can thus compete with L-Tyr in binding to TyrRS. In contrast to a classical competitive inhibitor, D-Tyr acts as a substrate of the enzyme, albeit with a sizable drop in catalytic efficiency. The A202V substitution destabilizes the binding of D-Tyr relative to L-Tyr, thereby increasing the stereoselectivity of the enzyme. We therefore conclude that $TyrRS^{A202V}$ has improved substrate specificity compared to $TyrRS^{WT}$.

Mutations in the *tyrS* riboswitch enhance *tyrS* expression. Synthesis of TyrRS is controlled by a T box riboswitch upstream of the *tyrS* open reading frame (26, 27). When L-Tyr is limiting, uncharged $tRNA^{Tyr}$ binds to the *tyrS* riboswitch at the specifier sequence (which contains the tyrosine codon UAC) as well as at the antiterminator region (28) (Fig. 4). This stabilizes the antiterminator hairpin, thereby allowing transcriptional readthrough from the riboswitch into *tyrS* and resulting in increased expression of *tyrS* (26, 27).

Our selection for resistance mutations yielded two mutations in the terminator hairpin of the *tyrS* riboswitch. We hypothesized that these mutations destabilize the terminator hairpin, $tyrS^{-38C>T}$, by causing a base pair mismatch (from C-G to C-A), and $tyrS^{-38\Omega C}$ by introducing a bulge into the hairpin (Fig. 4). We therefore expected that these *tyrS* riboswitch mutations would result in *tyrS* overexpression. Indeed, using a transcriptional fusion of the *tyrS* riboswitch to luciferase, we found that both mutations exhibited significantly higher luciferase activity than did the wild-type *tyrS* riboswitch (Fig. 5). These results

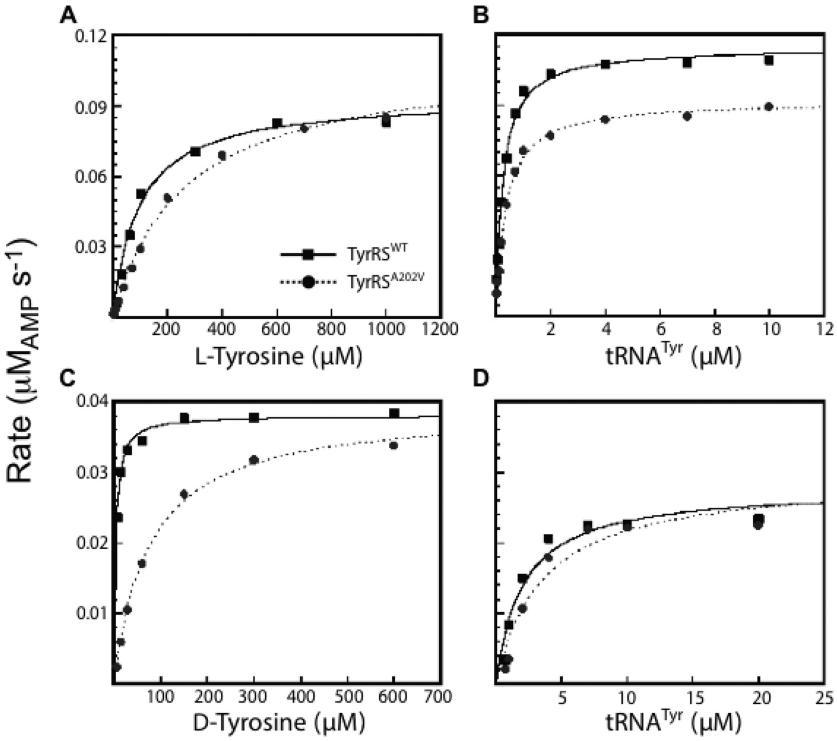

FIG 3 Representative steady-state kinetics of *B. subtilis* TyrRS. Representative data from eight independent trials are shown for the measurement of binding affinity (K_m) and turnover rate (k_{cat}) of wild-type TyrRS (TyrRS^{WT}) and mutant TyrRS (TyrRS^{A202V}) for L-Tyr, D-Tyr, and tRNA^{Tyr}. The experimental conditions were as follows: (A) 5 nM TyrRS and 2.5 μM tRNA^{Tyr}, (B) 5 nM TyrRS and 1 mM L-Tyr, (C) 125 nM TyrRS and 10 μM tRNA^{Tyr}, and (D) 125 nM TyrRS and 800 μM D-Tyr. All experiments included Mg-ATP at 10 mM. The results are summarized in Table 2.

suggest that *tyrS*$^{-38C>T}$ and *tyrS*$^{-38\Omega C}$ confer resistance to D-Tyr by increasing TyrRS levels in the cell.

The *trnD-Phe*$^{35A>T}$ mutation transforms tRNA^{Phe} into a *tyrS* riboswitch ligand. The recovery of a resistance mutation in *trnD*-Phe was surprising as *trnD*-Phe encodes a tRNA^{Phe}, and D-Phe was not used in our screen for D-amino acid-resistant mutations. Interestingly, however, the 35A>T mutation in *trnD*-Phe changes the tRNA^{Phe} anticodon from AAG (for L-Phe) to AUG (for L-Tyr). We also note that the sequence at the 3′ end of tRNA^{Phe} is identical to the corresponding sequence of tRNA^{Tyr} and that this sequence is known to base pair with the riboswitch antiterminator (29). Thus, tRNA^{Phe} with the AAG-to-AUG anticodon switch apparently contains both of the binding sites that dictate the tRNA^{Tyr}-*tyrS* riboswitch interaction (29) (Fig. 4). Moreover, the mutant tRNA^{Phe} has neither the proper recognition site for charging by phenylalanyl-tRNA synthetase nor that for charging by tyrosyl-tRNA synthetase, implying that the mutant tRNA^{Phe} is constitutively uncharged and available as a riboswitch ligand. We therefore postulated that the mutant tRNA^{Phe} also stimulates *tyrS* expression by interacting with the *tyrS* riboswitch. Consistent with our hypothesis is the complementary observation of Grundy and Henkin (26) that converting the *tyrS* riboswitch specifier sequence from UAC to UUC caused the *tyrS* riboswitch to become responsive to L-Phe limitation instead of L-Tyr limitation. As a test of our hypothesis, we measured *tyrS* expression using a transcriptional fusion of luciferase to the wild-type *tyrS* riboswitch. The results show that luciferase activity in the *trnD-Phe* mutant was significantly higher than that of the parental strain and, in fact, was similar to that observed for the two *tyrS* riboswitch mutants (Fig. 5). We also found that *tyrS* expression in the two *tyrS* riboswitch mutant strains and the *trnD-Phe* mutant strain was comparable to or greater than that observed for a mutant lacking the *tyrS* riboswitch terminator hairpin (Fig. 5). Notably, the *tyrS* riboswitch terminator and antiterminator hairpins share seven bases, and deletion of the terminator sequence affects the stability of the antiterminator conformation as well. It is therefore expected that luciferase expression driven by a *tyrS* riboswitch lacking the terminator hairpin will be below the level of constitutive expression. Thus, in summary, the *tyrS* riboswitch and *trnD-Phe* mutants studied here resulted in constitutive or near-constitutive *tyrS* expression.

TABLE 2 Steady-state kinetics of the TyrRS wild type and A202V variant

Enzyme and amino acid	Tyr		tRNA	
	K_m (μM)	k_{cat} (s^{-1})	K_m (μM)	k_{cat} (s^{-1})
TyrRS^{WT}				
L-Tyr	90 ± 20	14 ± 3	0.27 ± 0.05	15 ± 5
D-Tyr	4.0 ± 0.8	0.23 ± 0.04	2.2 ± 0.5	0.22 ± 0.01
TyrRS^{A202V}				
L-Tyr	260 ± 20	14 ± 4	0.42 ± 0.08	11 ± 5
D-Tyr	90 ± 20	0.27 ± 0.05	3.2 ± 0.8	0.23 ± 0.06

***tyrS* overexpression is sufficient to confer resistance to D-Tyr.** To confirm the causal relationship between *tyrS* overexpression and resistance to D-Tyr, we constructed derivatives of *B. subtilis* 3610 that harbor IPTG-inducible *tyrS* at the *amyE* locus.

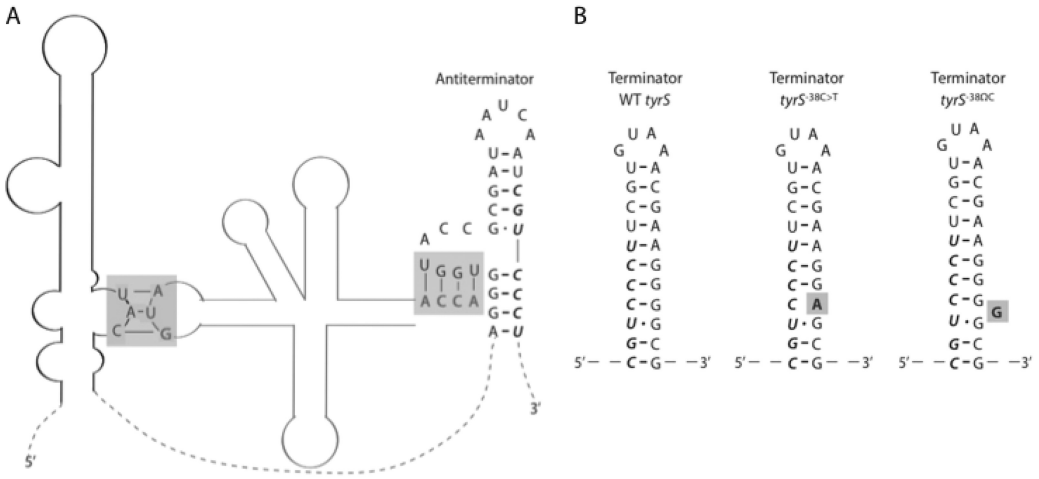

FIG 4 Schematic of the *B. subtilis tyrS* riboswitch. (A) The interaction sites of a $tRNA^{Tyr}$ (gray) with the *tyrS* riboswitch (black) are highlighted with gray boxes. The gray box on the left shows binding between the $tRNA^{Tyr}$ anticodon (AUG) and the riboswitch specifier sequence (UAC). The gray box on the right shows binding between the 3′-end sequence of the $tRNA^{Tyr}$ (ACCA) and the antiterminator. The mutant $tRNA^{Phe}$ resulting from *trnD-Phe*$^{35A>T}$ harbors the AUG anticodon as well as the ACCA sequence at its 3′ end and may therefore bind the *tyrS* riboswitch at the same locations as does $tRNA^{Tyr}$. Dashed lines represent riboswitch sequence that is not significant for binding $tRNA^{Tyr}$. (B) Comparison of the wild-type (WT) *tyrS* terminator hairpin with the proposed structures of mutant terminators. The relevant mutations are in bold and highlighted with gray boxes. In panels A and B, bases shown in italics are shared between the antiterminator and terminator hairpins. The secondary structures in panel A and the WT *tyrS* structure in panel B were originally depicted by Grundy et al. (28) and Gerdeman et al. (29).

Overexpression of the *tyrS* open reading frame yielded robust D-Tyr resistance (see Fig. S1 in the supplemental material). Overexpression of the *tyrS* riboswitch and open reading frame also yielded D-Tyr resistance, albeit to a lesser degree (see Fig. S1). This finding is consistent with evidence that the *tyrS* riboswitch normally occupies a terminator hairpin conformation, which would attenuate *tyrS* overexpression even in the presence of IPTG.

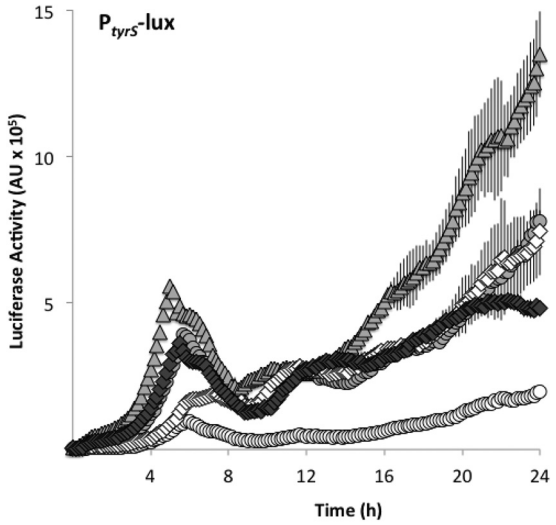

FIG 5 Mutations in the *tyrS* riboswitch and *trnD-Phe* cause readthrough. Expression of a luciferase transcriptional fusion to the *tyrS* riboswitch was measured in shaking MSgg medium. Riboswitch readthrough is indicated by white circles for the parental strain (SLH57) and by diamonds for the *trnD-Phe*$^{35A>T}$ mutant (SLH58). Luciferase fusions were also constructed with the *tyrS* riboswitch harboring either a C-to-T point mutation or an insertion mutation in the terminator hairpin. Readthrough of the *tyrS* riboswitch point mutant (SLH61) is shown as triangles, whereas readthrough of the insertion mutant (SLH59) is shown as gray circles. Readthrough of a *tyrS* riboswitch lacking the terminator hairpin sequence (SLH75) is indicated by white diamonds. Luciferase activity was determined by normalizing luminescence to optical density. Results shown are the averages from three replicates, and error bars show the standard deviations.

There are several possible explanations for how *tyrS* overexpression confers resistance to D-Tyr. While an excess of TyrRS would not change the ratio of proper charging to mischarging events, excess TyrRS would increase the absolute number of properly charged species. As such, excess TyrRS could help compensate for TyrRS sequestration by D-Tyr and thus increase the protein translation rate of D-Tyr-treated cells. Interestingly, excess TyrRS has been shown to cause erroneous tRNA charging in *E. coli* (30), implying that the benefits of excess TyrRS may be limited to *B. subtilis* or may be condition dependent.

An alternative explanation relates to the role of the *tyrS* riboswitch in sensing intracellular L-Tyr levels. Given that L-Tyr is a highly effective remedy for D-Tyr toxicity (12), either *tyrS* overexpression or the signals for *tyrS* overexpression (e.g., low L-Tyr or an accumulation of uncharged $tRNA^{Tyr}$) might result in D-Tyr resistance by stimulating the biosynthesis or import of L-Tyr. While such a feedback system exists for other amino acids, including L-Leu and L-Trp (31, 32), it has not been established whether L-Tyr levels can be similarly regulated. That said, changes in D-Tyr import and in L-Tyr production have been previously associated with D-Tyr resistance in *B. subtilis* (6, 33).

***tapA* mutations do not confer resistance to D-Tyr.** This laboratory previously reported that frameshift mutations in the 3′ region of the biofilm matrix gene *tapA* confer resistance to D-Tyr during biofilm formation (34).

This finding is at odds with our recent report that D-amino acids do not inhibit biofilm formation through their incorporation into peptidoglycan but that, rather, they do so via their incorporation into protein (12). In light of this evidence as well as our present identification of resistance mutations in genes involved in $tRNA^{Tyr}$ charging, we reexamined the reported effect of the *tapA*

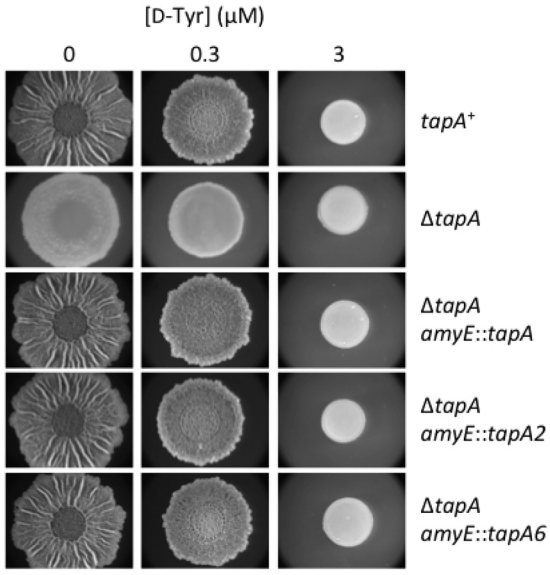

FIG 6 *tapA* mutations do not confer resistance to D-Tyr. A *B. subtilis* strain lacking the *tapA* operon (SLH63) was compared with a *tapA*$^+$ strain (3610) as well as with strains complemented at *amyE* for the *tapA* operon containing wild-type (SLH64) *tapA* or mutant *tapA* genes harboring the previously described frameshift mutation *tapA2* (SLH65) or *tapA6* (SLH66). All strains were spotted on solid MSgg medium lacking L-FTW and containing the indicated concentration of D-Tyr. Images were taken after 72 h of incubation at 30°C.

mutations *tapA2* and *tapA6*. We were unable to confirm the original *tapA2* and *tapA6* mutants and therefore reconstructed these strains using a derivative of strain 3610 lacking the *tapA-sipW-tasA* operon. The deletion of the native *tapA* operon was complemented with a copy of the operon inserted at the *amyE* locus that either was wild type for *tapA* or contained the *tapA2* or *tapA6* mutation. Each of the three complementation constructs restored wild-type matrix formation to untreated cells (Fig. 6). However, neither the *tapA2* nor the *tapA6* mutation rescued biofilm formation in the presence of D-Tyr under the conditions of Fig. 6 as well as at several other temperatures and under other nutrient conditions (data not shown). We conclude that the previously reported *tapA* mutations do not confer resistance to D-Tyr.

In summary, we have found that *B. subtilis* acquires resistance to D-Tyr through single mutations in protein-coding sequences or in regulatory regions of protein-coding sequences for genes that influence the fidelity of translation. Congenic resistance mutants revealed a hierarchy among the mutations according to their role in preventing the mischarging of tRNA^{Tyr} with D-Tyr. We found that the mutations that most specifically promoted the exclusion of D-Tyr from nascent protein (*tyrS*^{A202V}, *tyrS*$^{-38C>T}$, *tyrS*$^{-38\Omega C}$, and *trnD-Phe*$^{35A>T}$) were more effective at conferring resistance to D-Tyr during biofilm formation than were mutations in the pleiotropic gene *ppaC*. In agreement with our finding that D-amino acids influence biofilm formation only as a side effect of growth inhibition, we identified mutations that confer D-amino acid resistance in genes related to tRNA^{Tyr} charging but did not identify any resistance mutations relevant to biofilm formation or cell wall biosynthesis. We further showed that, in contrast to an earlier report, mutations in the biofilm gene *tapA* do not confer resistance to D-Tyr. An accompanying report reveals an additional mode of resistance involving the expression of a cryptic gene for a tyrosyl-tRNA synthetase (25).

ACKNOWLEDGMENTS

We thank the Bauer Core at Harvard University for assistance with whole-genome sequencing. We also thank Rebecca Williams-Wagner, Tina Henkin, and members of the Losick lab for helpful discussions.

Funding for this work was provided by the NIH (GM18568, to R. Losick), Louisiana State University Health Sciences Center in Shreveport, and the Biomedical Research Foundation of Northwest Louisiana.

REFERENCES

1. **Lam H, Oh DC, Cava F, Takacs CN, Clardy J, de Pedro MA, Waldor MK.** 2009. D-Amino acids govern stationary phase cell wall remodeling in bacteria. Science **325:**1552–1555. http://dx.doi.org/10.1126/science.1178123.
2. **Vollmer W, Blanot D, de Pedro MA.** 2008. Peptidoglycan structure and architecture. FEMS Microbiol Rev **32:**149–167. http://dx.doi.org/10.1111/j.1574-6976.2007.00094.x.
3. **Lupoli TJ, Tsukamoto H, Doud EH, Wang TS, Walker S, Kahne D.** 2011. Transpeptidase-mediated incorporation of D-amino acids into bacterial peptidoglycan. J Am Chem Soc **133:**10748–10751. http://dx.doi.org/10.1021/ja2040656.
4. **Ongena M, Jacques P.** 2008. *Bacillus* lipopeptides: versatile weapons for plant disease biocontrol. Trends Microbiol **16:**115–125. http://dx.doi.org/10.1016/j.tim.2007.12.009.
5. **Perego M, Glaser P, Minutello A, Strauch MA, Leopold K, Fischer W.** 1995. Incorporation of D-alanine into lipoteichoic acid and wall teichoic acid in *Bacillus subtilis*. Identification of genes and regulation. J Biol Chem **270:**15598–15606.
6. **Champney WS, Jensen RA.** 1969. D-Tyrosine as a metabolic inhibitor of *Bacillus subtilis*. J Bacteriol **98:**205–214.
7. **Champney WS, Jensen RA.** 1970. Molecular events in the growth inhibition of *Bacillus subtilis* by D-tyrosine. J Bacteriol **104:**107–116.
8. **Nandi N.** 2011. Chirality in biological nanospaces: reactions in active sites. CRC Press, London, United Kingdom.
9. **Calendar R, Berg P.** 1967. D-Tyrosyl RNA: formation, hydrolysis and utilization for protein synthesis. J Mol Biol **26:**39–54. http://dx.doi.org/10.1016/0022-2836(67)90259-8.
10. **Soutourina J, Blanquet S, Plateau P.** 2000. D-Tyrosyl-tRNA^{Tyr} metabolism in *Saccharomyces cerevisiae*. J Biol Chem **275:**11626–11630. http://dx.doi.org/10.1074/jbc.275.16.11626.
11. **Soutourina O, Soutourina J, Blanquet S, Plateau P.** 2004. Formation of D-tyrosyl-tRNA^{Tyr} accounts for the toxicity of D-tyrosine toward *Escherichia coli*. J Biol Chem **279:**42560–42565. http://dx.doi.org/10.1074/jbc.M402931200.
12. **Leiman SA, May JM, Lebar MD, Kahne D, Kolter R, Losick R.** 2013. D-Amino acids indirectly inhibit biofilm formation in *Bacillus subtilis* by interfering with protein synthesis. J Bacteriol **195:**5391–5395. http://dx.doi.org/10.1128/JB.00975-13.
13. **Harwood CR, Cutting SM.** 1990. Molecular biological methods for *Bacillus*. Wiley, Chichester, United Kingdom.
14. **Gibson DG, Young L, Chuang RY, Venter JC, Hutchison CA, III, Smith HO.** 2009. Enzymatic assembly of DNA molecules up to several hundred kilobases. Nat Methods **6:**343–345. http://dx.doi.org/10.1038/nmeth.1318.
15. **Branda SS, Chu F, Kearns DB, Losick R, Kolter R.** 2006. A major protein component of the *Bacillus subtilis* biofilm matrix. Mol Microbiol **59:**1229–1238. http://dx.doi.org/10.1111/j.1365-2958.2005.05020.x.
16. **Foulston L, Elsholz AK, DeFrancesco AS, Losick R.** 2014. The extracellular matrix of *Staphylococcus aureus* biofilms comprises cytoplasmic proteins that associate with the cell surface in response to decreasing pH. mBio **5**(5):e01667-14. http://dx.doi.org/10.1128/mBio.01667-14.
17. **Kleeman TA, Wei D, Simpson KL, First EA.** 1997. Human tyrosyl-tRNA synthetase shares amino acid sequence homology with a putative cytokine. J Biol Chem **272:**14420–14425. http://dx.doi.org/10.1074/jbc.272.22.14420.
18. **Gasteiger E, Gattiker A, Hoogland C, Ivanyi I, Appel RD, Bairoch A.** 2003. ExPASy: the proteomics server for in-depth protein knowledge and analysis. Nucleic Acids Res **31:**3784–3788. http://dx.doi.org/10.1093/nar/gkg563.
19. **Henkin TM, Glass BL, Grundy FJ.** 1992. Analysis of the *Bacillus subtilis tyrS* gene: conservation of a regulatory sequence in multiple tRNA synthetase genes. J Bacteriol **174:**1299–1306.
20. **Brick P, Bhat TN, Blow DM.** 1989. Structure of tyrosyl-tRNA synthetase

refined at 2.3 Å resolution. Interaction of the enzyme with the tyrosyl adenylate intermediate. J Mol Biol **208:**83–98.
21. **Halonen P, Tammenkoski M, Niiranen L, Huopalahti S, Parfenyev AN, Goldman A, Baykov A, Lahti R.** 2005. Effects of active site mutations on the metal binding affinity, catalytic competence, and stability of the family II pyrophosphatase from *Bacillus subtilis*. Biochemistry **44:**4004–4010. http://dx.doi.org/10.1021/bi047926u.
22. **Homuth G, Mogk A, Schumann W.** 1999. Post-transcriptional regulation of the *Bacillus subtilis dnaK* operon. Mol Microbiol **32:**1183–1197. http://dx.doi.org/10.1046/j.1365-2958.1999.01428.x.
23. **Sheoran A, Sharma G, First EA.** 2008. Activation of D-tyrosine by *Bacillus stearothermophilus* tyrosyl-tRNA synthetase: 1. Pre-steady-state kinetic analysis reveals the mechanistic basis for the recognition of D-tyrosine. J Biol Chem **283:**12960–12970. http://dx.doi.org/10.1074/jbc.M801649200.
24. **Tsunoda M, Kusakabe Y, Tanaka N, Ohno S, Nakamura M, Senda T, Moriguchi T, Asai N, Sekine M, Yokogawa T, Nishikawa K, Nakamura KT.** 2007. Structural basis for recognition of cognate tRNA by tyrosyl-tRNA synthetase from three kingdoms. Nucleic Acids Res **35:**4289–4300. http://dx.doi.org/10.1093/nar/gkm417.
25. **Williams-Wagner RN, Grundy FJ, Raina M, Ibba M, Henkin TM.** 2015. The *Bacillus subtilis tyrZ* gene encodes a highly selective tyrosyl-tRNA synthetase and is regulated by a MarR regulator and T box riboswitch. J Bacteriol **197:**1624–1631. http://dx.doi.org/10.1128/JB.00008-15.
26. **Grundy FJ, Henkin TM.** 1993. tRNA as a positive regulator of transcription antitermination in *B. subtilis*. Cell **74:**475–482. http://dx.doi.org/10.1016/0092-8674(93)80049-K.
27. **Wang J, Nikonowicz EP.** 2011. Solution structure of the K-turn and specifier loop domains from the *Bacillus subtilis tyrS* T-box leader RNA. J Mol Biol **408:**99–117. http://dx.doi.org/10.1016/j.jmb.2011.02.014.
28. **Grundy FJ, Hodil SE, Rollins SM, Henkin TM.** 1997. Specificity of tRNA-mRNA interactions in *Bacillus subtilis tyrS* antitermination. J Bacteriol **179:**2587–2594.
29. **Gerdeman MS, Henkin TM, Hines JV.** 2002. In vitro structure-function studies of the *Bacillus subtilis tyrS* mRNA antiterminator: evidence for factor-independent tRNA acceptor stem binding specificity. Nucleic Acids Res **30:**1065–1072. http://dx.doi.org/10.1093/nar/30.4.1065.
30. **Bedouelle H, Guez V, Vidal-Cros A, Hermann M.** 1990. Overproduction of tyrosyl-tRNA synthetase is toxic to *Escherichia coli*: a genetic analysis. J Bacteriol **172:**3940–3945.
31. **Grundy FJ, Henkin TM.** 1994. Conservation of a transcription antitermination mechanism in aminoacyl-tRNA synthetase and amino acid biosynthesis genes in gram-positive bacteria. J Mol Biol **235:**798–804. http://dx.doi.org/10.1006/jmbi.1994.1038.
32. **Shimotsu H, Henner DJ.** 1984. Characterization of the *Bacillus subtilis* tryptophan promoter region. Proc Natl Acad Sci U S A **81:**6315–6319. http://dx.doi.org/10.1073/pnas.81.20.6315.
33. **Jensen RA, Stenmark SL, Champney WS.** 1972. Molecular basis for the differential anti-metabolite action of D-tyrosine in strains 23 and 168 of *Bacillus subtilis*. Arch Mikrobiol **87:**173–180. http://dx.doi.org/10.1007/BF00424998.
34. **Kolodkin-Gal I, Romero D, Cao S, Clardy J, Kolter R, Losick R.** 2010. D-Amino acids trigger biofilm disassembly. Science **328:**627–629. http://dx.doi.org/10.1126/science.1188628.